# APPLICATIONS OF PROTON AND CARBON-13 NUCLEAR MAGNETIC RESONANCE TO THE STUDY OF MOLECULAR TRANSLATION IN LIQUID SOLUTION

A THESIS

Presented to

The Faculty of the Division of Graduate

Studies and Research

By

Robert Lee Harris, Jr.

In Partial Fulfillment

of the Requirements for the Degree

Master of Science in Chemistry

Georgia Institute of Technology

June, 1974

# APPLICATIONS OF PROTON AND CARBON-13 NUCLEAR MAGNETIC RESONANCE TO THE STUDY OF MOLECULAR TRANSLATION IN LIQUID SOLUTION

Approved:

S. L. Gordon, Chairman

R. F. Borkman

R. H. Felton

Date approved by Chairman: 5/20/74

# ACKNOWLEDGMENTS

I wish to express my gratitude to Dr. S. L. Gordon for his inspiration, guidance, and friendship.

The Department of the Army is to be thanked for affording me the opportunity to pursue graduate studies. Partial support for my research was provided by the National Science Foundation.

The advice and assistance of Mr. Don Lillie in fabrication of glassware and Mr. James Horton III in the operation of the JEOL PFT-100 NMR Spectrometer are gratefully acknowledged.

TABLE OF CONTENTS

# LIST OF TABLES

# LIST OF ILLUSTRATIONS

## SUMMARY

The proton nuclear spin-lattice relaxation times are measured for a series of binary haloform solutions. The measurements are made as a function of mole fraction solute. The spin-lattice relaxation times are obtained from the decay curves. Measurements are made on the JEOL 4H-100 and PFT-100 NMR Spectrometers.

The haloform molecules are massive enough that only dipolar relaxation should occur and since each molecule has only one proton, all dipolar relaxation is intermolecular. The intermolecular dipole-dipole mechanism depends upon the relative translational correlation times and the distances of closest approach and as such is one of the few experimental parameters that depend directly on intermolecular pair interactions in solutions. The results are compared to a statistical model for relaxation in an ideal solution. The comparison is then used to establish that as the solutions become enriched in chloroform, the molecules see a microviscosity rather than the bulk viscosity.

The proton - carbon-13 intermolecular Nuclear Overhauser enhancements (NOE) and carbon-13 spin-lattice relaxation times are measured in a solution of 0.2 mole fraction deuterated acetone in water. Measurements are made on the JEOL PFT-100 Fourier Transform NMR Spectrometer. The

NOE values are obtained using a carbon tetrachloride external reference. The carbon-13 relaxation times are measured using the partially relaxed fourier transform method.

The NOE values and the relaxation times are used to determine the intermolecular relaxation rates for the carbonyl and the methyl carbons of the acetone. These rates are used to show that the solvent is interacting more strongly with the carbonyl part of the molecule.

# CHAPTER I

## INTRODUCTION

The tremendous advances in Nuclear Magnetic Resonance (NMR) equipment in recent years make it highly desirable to find new ways to use NMR spectroscopy data. One such aspect is relaxation studies. Determination of experimental relaxation rates can give insights into molecular interactions. The total relaxation rate of a molecule is the sum of several individual and distinct rates.[1] Isolation of the different rates is desirable because each is the result of a different type of molecular interaction. Of particular interest in this work is the dipole-dipole interaction. A dipolar interaction can occur between two protons (homonuclear interaction) or between two different magnetic species such as a proton and a carbon-13 (heteronuclear interaction).

There are two types of dipolar relaxation. Intramolecular relaxation is caused by the reorientation of the molecule and can be used to determine the reorientational correlation time. Intermolecular dipolar relaxation is caused by molecular translation and can be used to study the relative translational correlation time and the distance of closest approach. The latter interaction is one of the few

experimental parameters for liquids which depend directly on intermolecular pair interactions and is the subject of interest in these studies.

Early relaxation studies were thought to have shown that at room temperature proton spin-lattice relaxation times of simple molecules were determined mainly by dipolar interactions.[2] More recent results by Krishna have shown this to be untrue and pointed out that spin rotation is important. His experiments on methylene dibromide showed that the relaxation was 20 percent spin rotation.[3] Krishna, et al., earlier did intermolecular proton dipole-dipole studies on systems where there were competing mechanisms due to the intramolecular dipole-dipole interactions.[4]

The choice of the haloforms for this study provided molecules that have a larger moment of inertia and thus rotate more slowly; the resultant smaller molecular magnetic moment might eliminate spin rotation relaxation. This prediction proved to be true and the molecules displayed only dipolar relaxation. The binary haloform solutions had only one proton per molecule and thus no possibility of intramolecular relaxation. In these solutions it is possible to study directly the correctness of the basic formulism for intermolecular relaxation and to study the sensitivity of the experiment to molecular parameters such as the relative translational correlation time and the distances of closest approach. The proton spin-lattice

relaxation times of various concentrations of bromoform-chloroform solutions and iodoform-chloroform solutions were measured. This is different from other investigations of the molecules in which each haloform was examined individually in a carbon disulfide medium.[2] The results are discussed in terms of the individual properties of the molecules and their interactions in solution. Then the experiments could be extended to larger molecules and a proton-carbon-13 relaxation mechanism could-be investigated. Prior to this work the intermolecular relaxation process in carbon-13 experiments had not been observed.

Proton-carbon-13 dipolar interactions in acetone-d6-water solutions were studied. Interpretation of the results is complicated by spin-rotation relaxation of carbon-13. However, it was possible to see substantial intermolecular dipolar contributions to the total relaxation mechanism because of the Nuclear Overhauser Effect (NOE). The NOE magnifies the intermolecular dipolar relaxation by a factor of four ($\gamma_{1_H}/\gamma_{13_C} \simeq 4$).

It is hoped that these studies will lead to a practical technique for mapping the relative translational velocities between each pair of nuclei (i.e. each carbon-13 of a molecule and the protons surrounding it) in the solution and provide detailed information about the collision processes that occur in the solution.

In Chapter II the relaxation mechanisms of interest

and the theory behind them are discussed. The Nuclear Overhauser Effect is explained in detail.

Chapter III details the experimental results obtained for the binary haloform solutions and discusses them in terms of the dipolar relaxation process. An attempt is made to interpret the results in terms of a simple model. Chapter IV gives the results of the proton-carbon-13 experiments and discusses the problems occuring in trying to obtain relevant data.

# CHAPTER II

## NUCLEAR RELAXATION THEORY

The nuclear magnetization of a sample, $\underset{\sim}{M}$, is the sum of all the individual nuclear magnetic moments, $\underset{\sim}{\mu}$, per unit volume of sample. Spin $\frac{1}{2}$ nuclei in a dc magnetic field, $\underset{\sim}{H}_o$, can be in two spin states with magnetic quantum numbers $+\frac{1}{2}$ and $-\frac{1}{2}$, and energies $-\mu_z H_o$ and $+\mu_z H_o$, respectively. The lower level energy corresponds to u aligned parallel to $\underset{\sim}{H}_o$ and the higher level energy to the antiparallel alignment.[5]

An oscillating magnetic field, $\underset{\sim}{H}$, can cause transitions between the two nuclear spin levels. This field can produce transitions in either direction with equal probability per nucleus per unit time. However, at equilibrium, the population of the lower level exceeds that of the upper level according to the Boltzmann distribution law, and there is a net absorption of energy. It might seem that the rf field would soon cause the populations to become equal with no more energy being absorbed. This, in fact, will happen if the rf field strength is large enough. This is called saturation. However, there is a process which opposes the equalization of the populations by $\underset{\sim}{H}$. This process is the exchange of energy between the translational, rotational, and vibrational degrees of freedom (the lattice) and the

nuclear spins. This process is called spin-lattice relaxation. The coupling which causes the energy transfer between the nuclear system and the lattice depends upon the fluctuating localized magnetic fields at the sites of the nuclei. The spin-lattice coupling is characterized by a relaxation rate $R_1$, which can be determined from the measurement of the spin-lattice relaxation time, $T_1$. The stronger the spin-lattice relaxation is, the shorter the characteristic $T_1$, and vice-versa.[1,6]

At equilibrium, the energy levels have populations $p_i^o$ given by[6]

$$P_i^o = K \exp(-E_i/kT), \tag{1}$$

where $E_i$ is the energy of the $i^{th}$ level and K is a normalization constant. If at time zero, the populations have a non-Boltzmann distribution, $P_i$ will approach $P_i^o$ according to

$$dP_i/dt = \sum_j W_{ji}(P_j - P_j^o) - \sum_j W_{ij}(P_i - P_i^o), \tag{2}$$

where $W_{ij}$ and $W_{ji}$ are the thermal transition probabilities from levels i to j and levels j to i, respectively.[6]

First, let us look at a single spin case relaxing in an external random field. Take a sample of protons or carbon-13 and call $P_1$, the population of the $+\frac{1}{2}$ state and $P_2$ the population of the $-\frac{1}{2}$ state. In addition, neglect

the small difference between $W_{12}$ and $W_{21}$, and let W be equal to $\frac{1}{2}(W_{12} + W_{21})$. Then,

$$dP_1/dt = -W(P_1-P_1^o) + W(P_2-P_2^o), \tag{3}$$

and

$$dP_2/dt = -W(P_2-P_2^o) + W(P_1-P_1^o). \tag{4}$$

If equation (3) is subtracted from equation (4) and the difference rearranged, we get

$$d(P_1-P_2)/dt = -2W(P_1-P_2) + 2W(P_1^o-P_2^o). \tag{5}$$

But, $M_z = nu_z(P_1-P_2)$, where n is the number of nuclei per unit volume. Therefore,

$$dM_z/dt = nu_z\ d(P_1-P_2)/dt, \tag{6}$$

and from (6)

$$dM_z/dt = -2W\ [M_z(t) - M_z(\infty)], \tag{7}$$

where $M_z(\infty)$ is the equilibrium value of $M_z(t)$. The time $T_1$ is defined as the time constant for an exponential recovery curve of $M_z$ and is seen as the experimental

exponential decay rate. Therefore,

$$T_1 = 1/2W, \tag{8}$$

and the solution to (7) becomes

$$M_z(t) = e^{-t/T_1} [M_z(0) - M_z(\infty)] + M_z(\infty), \tag{9}$$

with $M_z(0)$ being the initial value of $M_z(t)$.

Some of the relaxation mechanisms which can be important for nuclear spin-lattice relaxation are dipole-dipole, spin-rotation, chemical shift anisotropy, and scalar coupling to a chemically exchanging or quadrupolar relaxing nucleus.[1]

The dipole-dipole interaction between nuclei is of specific interest in these experiments. To correctly describe dipolar relaxation one needs to consider the relaxation of two spins. There are two types of dipole-dipole interactions and it is important to distinguish between them. First, there is intramolecular dipole-dipole (dd). The intramolecular dipole-dipole relaxation is caused by local magnetic fields which are due to other magnetic nuclei in the same molecule. The relaxation between the carbon-13 and a proton of a $^{13}CHCl_3$ molecule is an example of an intramolecular interaction. The other type of dipole-dipole interaction is intermolecular (xd). This

is the interaction between magnetic nuclei of one molecule and the magnetic nuclei of another molecule nearby. The relaxation process between a carbon-13 in acetone and the protons of an $H_2O$ solvent molecule is an intermolecular process.

Let us now extend the formulation to the case of two nuclei relaxing each other by dipole-dipole interactions. If we have two spins $\frac{1}{2}$, $I = S = \frac{1}{2}$, there are four possible energy levels which will be labeled as in Figure 1.[1] Then,

$$\langle I_z \rangle = \frac{1}{2}(P_1 + P_2 - P_3 - P_4), \tag{10}$$

and

$$\langle S_z \rangle = \frac{1}{2}(P_1 - P_2 + P_3 - P_4), \tag{11}$$

where $M_z(I) = n_i u \langle I_z \rangle$ and $M_z(S) = n_s u \langle S_z \rangle$. Therefore,

$$d\langle I_z \rangle/dt = \frac{1}{2}(dP_1/dt + dP_2/dt - dP_3/dt - dP_4/dt), \tag{12}$$

and

$$d\langle S_z \rangle/dt = \frac{1}{2}(dP_1/dt - dP_2/dt + dP_3/dt - dP_4/dt). \tag{13}$$

Using equation (2) and substituting into equation (20) and (21) gives

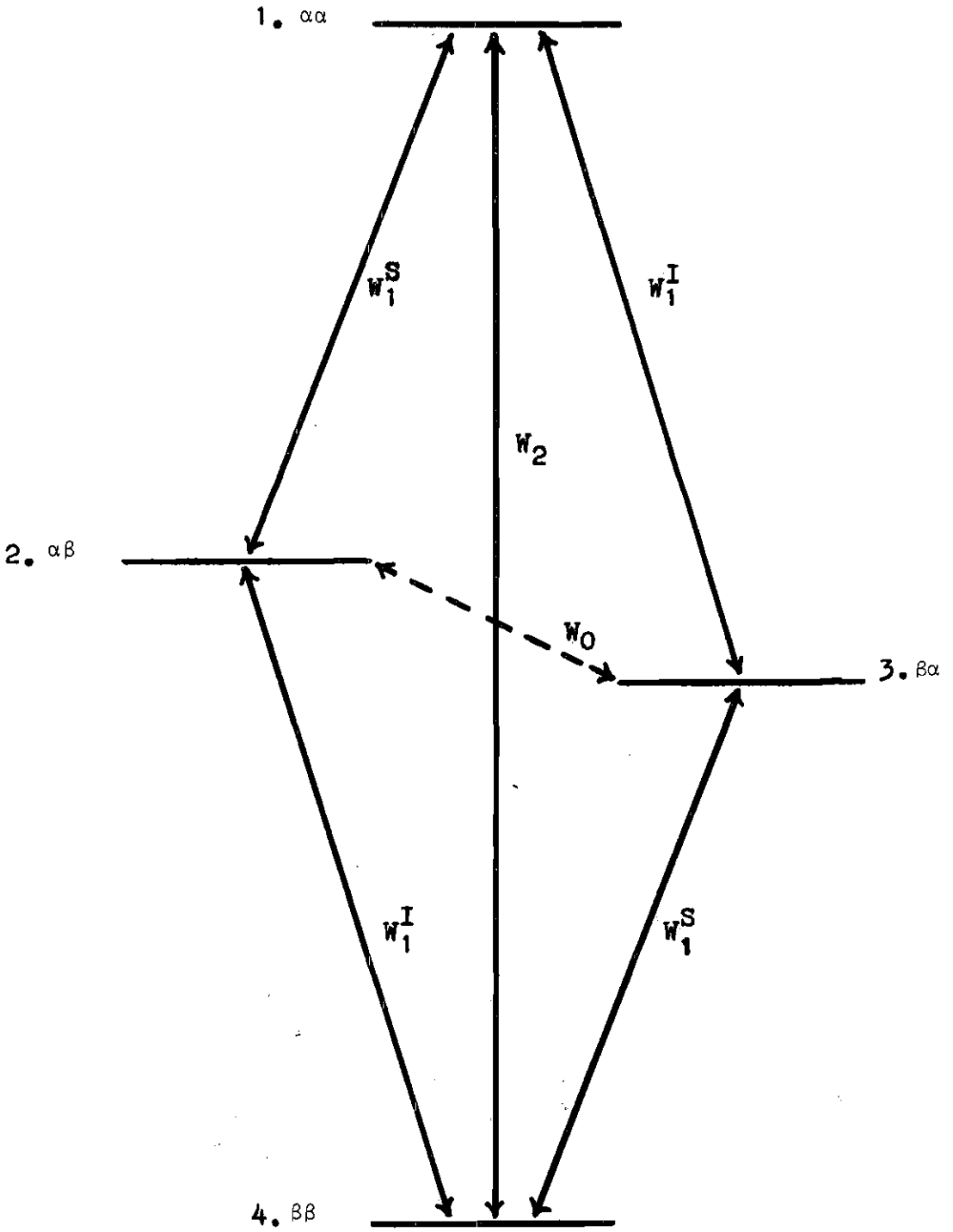


Figure 1. Energy Level Diagram For Two Spins $\frac{1}{2}$

$$d\langle I_z\rangle/dt = -2W_1^I[\langle I_z\rangle - I_o] - W_o[(P_2 - P_2^o) - (P_3 - P_3^o)]$$

$$- W_2[(P_1 - P_1^o) - (P_4 - P_4^o)], \qquad (14)$$

and

$$d\langle S_z\rangle/dt = -2W_1^S[\langle S_z\rangle - S_o] + W_o[(P_2 - P_2^o) + (P_3 - P_3^o)]$$

$$- W_2[(P_1 - P_1^o) + (P_4 - P_4^o)]. \qquad (15)$$

This is possible because in the weak coupling limit,[1] $W_1^I = W_{13} = W_{24}$, $W_1^S = W_{12} = W_{34}$, $W_o = W_{23}$ and $W_2 = W_{14}$, where $W_1^I$ is the single quantum transition probability for spin I, $W_1^S$ is the single quantum transition probability for spin S, $W_o$ is the zero quantum transition probability for both spins, and $W_2$ is the two quantum transition probability for the spins to relax in the same direction at the same time.

Adding and subtracting equations (10) and (11),

$$\langle I_z\rangle + \langle S_z\rangle = P_1 - P_4, \qquad (16)$$

and

$$\langle I_z\rangle - \langle S_z\rangle = P_2 - P_3. \qquad (17)$$

Therefore,

$$d\langle I_z\rangle/dt = -1/T_1^{II}[\langle I_z\rangle - I_o] - 1/T_1^{IS}[\langle S_z\rangle - S_o], \qquad (18)$$

and

$$d\langle S_z\rangle/dt = -1/T_1^{SS}[\langle S_z\rangle - S_o] - 1/T_1^{SI}[\langle I_z\rangle - I_o], \qquad (19)$$

where

$$1/T_1^{II} = 2W_1^I + W_o + W_2, \qquad (20)$$

$$1/T_1^{SS} = 2W_1^S + W_o + W_2, \qquad (21)$$

and

$$1/T_1^{IS} = 1/T_1^{SI} = W_2 - W_o. \qquad (22)$$

It is the cross relaxation terms (the second terms) in equation (18) and (19) which are responsible for the Nuclear Overhauser Enhancement. If we saturate spin I at its Larmor frequency, then $\langle I_z\rangle = 0$, and we obtain an enhancement of $\langle S_z\rangle$ compared to its equilibrium value $S_o$. This enhancement experimentally is defined by[3]

$$\eta = (\langle S_z\rangle - S_o)/S_o. \qquad (23)$$

When the steady state is reached, $d\langle S_z\rangle/dt = 0$, and equation (32) gives[1]

$$\eta = (S_o/T_1^{IS})/(I_o/T_1^{II}). \tag{24}$$

Knowing the total spin quantum numbers, S and I, and the gyromagnetic ratios, $\gamma_S$ and $\gamma_I$, of S and I, respectively, gives

$$\eta = \gamma_S \frac{1}{T_1^{IS}} S(S+1)/\gamma_I \frac{1}{T_1^{II}} I(I+1). \tag{25}$$

The gyromagnetic ratios are very important for NOE, especially for different species of nuclei. The I and S factors in $(1/T_1^{IS})/(1/T_1^{II})$ cancel. Most Overhauser experiments will be on nuclei of spin $\frac{1}{2}$. Therefore equation (25) can be further reduced to

$$\eta = \frac{W_2 - W_0}{2W_1^I + W_0 + W_2}. \tag{26}$$

If spin S relaxes only by dipole-dipole interactions, $W_2:W_1:W_0 = 12:3:2$,[1] and

$$\frac{1}{T_1^{SI}}/\frac{1}{T_1^{II}} = S(S+1)/2I(I+1), \tag{27}$$

and

$$\eta = \frac{\gamma_S}{2\gamma_I}, \tag{28}$$

The enhancement factor $\eta$ depends only on the gyromagnetic ratios, and represents the maximum enhancement possible. Other relaxation processes will contribute to $T_1$ but the $(1/T_1)$ dipole-dipole can be calculated by[7]

$$\frac{\eta(\text{observed})}{\gamma_S/2\gamma_I} \times \frac{1}{T_1}\text{total} = \frac{1}{T_1}\text{dipole-dipole} \tag{29}$$

Formulas have been derived to determine the dipolar relaxation rates. They are not exact but can be used to give predictions for experimental rates and give an insight into the parameters upon which the relaxation depends. Solomon derived a formula for $T_1$ for the intramolecular dipole mechanism for nonequivalent nuclei in terms of the rotational correlation time $\tau_c$ of the molecule in the liquid,[8]

$$1/T_1 = h^2\gamma^2\gamma'^2/b^6, \tag{30}$$

where b is the internuclear distance. For equivalent nuclei of the same species, Solomon obtained

$$1/T_1 = \frac{\frac{3}{2} h^2\gamma^4}{b^6} \tau_c. \qquad (31)$$

Bloembergen, Purcell, and Pound, using a spherical model derived a formula for the rotational correlation time,

$$\tau_c = \frac{4\pi\eta a^3}{3kT}, \qquad (32)$$

where $\eta$ is the viscosity and a is the radius of the sphere.[5] Gutowsky and Woessner extended this to get results for both the intermolecular and the intramolecular contributions to $T_1$. Of interest is their formula for the former,

$$\frac{1}{T_{1i}} = \frac{\pi^2 h^2 \gamma_i^2 \eta N_o a}{kT} \left(3\gamma_i^2 \sum_j \frac{1}{r_{ij}} + 2\sum_f \gamma_f^2 \frac{1}{r_{if}^o}\right), \qquad (33)$$

where i is the nucleus of interest, j are nuclei of the same species, and f all other nuclei, $r_{ij}^o$ is the mean value of $r_{ij}$ for two molecules in contact, $N_o$ the number of molecules per unit volume, and a is the radius of the sphere.[9]

Equation (33) was refined to use Gierer's micro-viscosity formula for the diffusion constant[10]

$$D\ (\text{trans}) = kT/6\pi\eta a f_t \qquad (34)$$

where

$$f_t = (3r_s/2r_o) + [1/(1 + r_s/r_o)] \tag{35}$$

for a spherical molecule of radius, $r_o$, in a solvent of radius, $r_s$, and viscosity $\eta$. This replaces the Stokes-Einstein relation $D = kT/6\pi\eta a$ in equation (33) and if $D_{IS} = \frac{1}{2}(D_I + D_S)$, then (33) can be written for two nuclei as approximately[1]

$$\frac{1}{T_{inter}} = \frac{8\pi}{45} N_s \gamma_s^2 \gamma_I^2 h^2 S(S+1)/D_{IS}a \tag{36}$$

Given the experimental $(1/T_1)^{xd}$ and (34) which is a good approximation of the diffusion constant, it is straightforward to calculate an approximation for a, the distance of closest approach. It should be noted that this model assumes that the proton is at the center of the molecule.

Pople, Schneider, and Bernstein use the Stokes-Einstein equation and assume equal gyromagnetic ratios and spins to get[11]

$$1/T_{inter} = \frac{3\pi^2 \gamma^4 h^2 \eta No}{kT} \tag{37}$$

This formula just like all of the other formulas for the relaxation rate assumes spherical molecules in that the

distance of closest approach is independent of the relative orientations of the molecules during a collision. An attempt to drop this assumption is made while trying to interpret experimental results.

# CHAPTER III

# INSTRUMENTATION, SAMPLE PREPARATION, AND EXPERIMENTAL PROCEDURES

## Sample Preparation

The chloroform (99.9%) and carbon tetrachloride (99.9%) were obtained from the Fisher Scientific Company. The Bromoform (99%) was purchased from the Eastman Kodak Company. The tetramethylsilane (99.9%) and the chloroform-d1 (99.8%) were obtained from Nuclear Magnetic Resonance Specialties, Incorporated. The acetone-d6 (99.6%) was purchased from Merck Sharp and Dohme of Canada Limited. Deuterium oxide (99.7%) from Diaprep Incorporated was used. All NMR tubes and caps were manufactured by the Wilmad Company.

The method of degassing used was to subject the sample to a series of freeze-pump-thaw cycles. The desired solutions were put directly into an NMR sample tube which had been fused to an adaptor to fit the vacuum system. Five millimeter tubes were used for experiments on proton-proton relaxation and either eight millimeter or ten millimeter tubes were used for the carbon-13 experiments. The sample was then attached to the vacuum system. Then the sample was frozen using liquid nitrogen. The frozen sample was opened

to the vacuum system and the system evacuated until a pressure of $10^{-5}$ torr was reached. The sample was then closed off from the vacuum system and allowed to thaw. This cycle was repeated a minimum of seven times. Additional cycles were used if air bubbles continued to rise to the surface during the thawing process, after the seventh evacuation. After sufficient degassing cycles were performed, the sample was then sealed and removed.

For samples used in the carbon-13 experiments, the sealed eight millimeter tube was placed into a ten millimeter tube which contained a reference substance. Sufficient reference material had to be present in the larger tube to entirely surround the smaller tube to a height above the level of the coil. The larger tube was then capped with a standard plastic pressure cap. To insure that this smaller tube did not wobble during spinning, it had to be firmly resting on the bottom of the larger tube. This was accomplished either by the cap of the larger tube holding it down or by the cap and packing material holding it down. Folded filter paper served as adequate packing material.

## Proton $T_1$ Measurement Procedure

According to equation (9) the magnetization increases towards its equilibrium value exponentially with time constant $T_1$. For the signal to increase according to (9), the observing rf field $H_1$ must not be too large or it will

saturate the spin system. In the direct method of experimentation the spin system is irradiated by a strong rf field. The rf field is then reduced to a non-saturating value and the signal is periodically sampled. The recovery of the absorption signal will then follow equation (9).

Measurements were made using JEOL 4H-100 and JEOL PFT-100 spectrometers. The time curves were recorded on the spectrometer recorder. Measurements were made by periodically recording the resonance line using a saw tooth sweep. The display was adjusted to a convenient height using the amplitude control and the attenuator on the spectrometer console. The signal was recorded 15 times. The rf level was increased by six db and another 15 sweeps were taken. If the peak height doubled, then the sample was not being saturated at the original rf level. Once that it was assured that the signal was not being saturated, the signal was recorded at least ten times to provide a value for the equilibrium height. Then the magnetization was inverted by adiabatic fast passage. After inversion, the power was reduced to normal and the signal recorded as a function of time. It is essential that the main magnetic field be kept sufficiently inhomogeneous or the line will be too narrow. This problem was minimized by not spinning the sample in the probe. This broadened the line and made the signal less sensitive to the field homogeneity.

The experimental sweep time was determined by timing

a fixed number of sweeps and then dividing the elapsed time by the number of sweeps to give a time period. Experiments were run with a minimum interval of five $T_1$'s between runs. Six runs were made per sample. The decay was assumed to be exponential and to follow equation (9). The $T_1$ value was found using a program written for the Wang 700 calculator. The program was written to take a maximum of 19 points. Values for N (number of points), $S_\infty$, and $\tau$ are put into the data bank. Values for S(t) from 1 to N are fed into the calculator. The program outputs values for $T_1$, the intercept on the t-axis, and the RMS deviation. The program was written to use the method of least squares to fit the data to ($y = mx + b$). Six values for each sample were computed and the average taken.

The direct method is relatively simple, is readily interpreted, and is easy to visualize. It required no modification of the standard spectrometers. The $T_1$ of individual lines of the overall NMR spectrum can be determined. The sensitivity of the method is limited by the steady-state nature of the experiment.

## NOE Measurements on PFT-100

Fourier Transfrom NMR was developed to increase the signal to noise (S/N) ratio for experiments where the magnetic nuclei to be examined were of low concentration. This has proved to be tremendously beneficial in carbon-13

NMR because this isotope has a natural abundance of 1.1 percent.[7]

The process of FT NMR starts with data accumulation in the form of free induction decay (FID) curves. The accumulated FID is multiplied by an apodization exponential and stored. Next the FID is fourier transformed. After phase corrections the FT spectrum is displayed on the oscilloscope and plotted by the recorder.[12,13]

The FID are accumulated in order to improve the signal to noise ratio. This is very important in carbon-13 NMR spectroscopy. The purpose of the window function is to further improve the S/N ratio by elimination of some of the noise at the lower end of the FID. The FID is in the time domain. The FT converts this from the time domain into the frequency domain. The latter is nothing more than a standard NMR absorption spectra.

The accurate measurement of the NOE of the carbonyl and the deuterated methyl peaks required a reference that would not be enhanced and preferably would not be subject to coupling. If the reference was in the same tube as the molecules it would be subject to intermolecular NOE from the protons of the solvent. Carbon tetrachloride was found to serve as an adequate reference because it gives a strong signal, contains no protons to cause intermolecular NOE, and has a boiling point high enough so that there is no concern with evaporation during long term accumulations. In all of

the experiments the deuterated acetone provided the required lock material for the deuterium lock.

An increase in the number of scans increases the S/N ratio as the square root of N. Thus a large number of scans for each experiment is preferable but not always possible. The number of scans used for each experiment was dependent upon the availability of the spectrometer. The excellent lock which was able to be obtained in the experiments due to the abundance of deuterium made overnight long term accumulations possible when the instrument was available. Care was taken however to insure that the number of scans for the non-decoupled and the decoupled parts of each individual experiment were the same and that the two were run consecutively.

The fourier transform experiments used an 8192 point transform and a 6250 hertz bandwidth. This gave a computer resolution of 1.526 hertz. An exponential minus three window processing was used for the FID. The $\pi/2$ pulse was provided by a single pulse width setting of 22 microseconds. The repetition time between pulses was 200 seconds. Once an adequate lock was obtained and the parameters set, the program was entirely automatic.

## Carbon-13 $T_1$ Measurements Procedure

The carbon-13 $T_1$ measurements on the FT spectrometer were performed using an automatic program. It was written

to observe the FID following the 90 degree pulse in a pulse sequence of 180° - t - 90° with t variable.[7] The values for t are set by the programmer but all of the basic parameters remain the same as in the previous section. The values for t used were $t = t_o + n\Delta t$ with n being consecutive integers. It should be noted that the $T_1$ program written for the spectrometer does not require the values of t to be separated by an equal time interval but it was done for these experiments so that the $T_1$ computed by the spectrometer could be checked on the Wang 700. The spectrometer prints out the various heights at each value of t and the value for $T_1$ of each individual peak.

# CHAPTER IV

## PROTON INTERMOLECULAR DIPOLAR RELAXATION IN BINARY HALOFORM SOLUTIONS

The binary haloform solutions chosen for these experiments are systems where intermolecular dipolar relaxation is believed to be the only relaxation mechanism present. They thus provide a system where information about the fundamental collision process of the molecule in solution can be derived. Of interest here are the relative translational motions and the distances of closest approach.

Since the three haloforms studied had only one proton they each gave only one NMR signal. Therefore, each binary system had two signals. Bromoform and chloroform were the easiest to work with as they are both liquids at room temperature and are completely miscible in each other. Their NMR chemical shifts are separated by 42 hertz. However, their relaxation times are quite different, 84 seconds for neat chloroform and 22 seconds for neat bromoform.[2] Iodoform is a solid at room temperature and not very soluble in chloroform. The chloroform and iodoform peaks are separated by approximately 200 hertz. The low solubility of iodoform made the signal to noise ratio very small for the iodoform signal.

Two experiments were run on each sample. Experiment A consisted of inverting the magnetization of the solute alone while the solvent remained at thermal equilibrium. Experiment B entailed an inversion of both the solute and solvent signal, at the same time. Experiment B was relatively simple to perform, but there was some difficulty in performing Experiment A. The closeness of the bromoform and chloroform signals made it difficult to invert the magnetization of the solute without disturbing the magnetization of the solvent. This problem did not occur with the iodoform-chloroform solutions because the signals were well separated.

The magnetization is inverted by sweeping through resonance with a strong rf field as explained in Chapter II. This is called adiabatic rapid passage. If time zero is the time of inversion, then $M_z(t=0)$ should be equal to $-M_\infty$. However, in reality it does not go to $-M_\infty$ because inversion is not total. The decay back to the $M_\infty$ value was assumed to be exponential and follow equation (9). The experimental $T_1$ is just the time constant of this exponential decay. If the logarithm of $M_z(t) - M_\infty$ is plotted versus t, the slope equals $-1/T_1$. The fact that the slope is not dependent upon the choice of origin enables one to disregard the first peak after inversion. This peak is generally invalid. The $M_z$ values are proportional to the intensities of the peaks.

For small molecules containing only one proton, the dipole-dipole contribution will be entirely intermolecular

and described by equation (18). In experiment B where the solute and solvent are both disturbed from thermal equilibrium, the relaxation rate is due to both terms in the equation. When only the solute signal is inverted and the solvent remains at thermal equilibrium, the measured rate is due to only the first term in equation (18). The term $(S_z - S_o)$ is zero in this case and the second term of the equation drops out. The maximum increase in the solute relaxation rate that can occur due to the "boost" from the solvent relaxation is 50%. This will occur at infinite dilution of solute provided the relaxation is entirely due to dipolar interaction. At the other extreme of neat solute the rates of experiments A and B should be equal because the second term is zero.

Equation (37) shows that in the bromoform-chloroform solutions only the viscosity, $\eta$, the molecules per unit volume, $N_o$, and the distance of closest approach influence the intermolecular relaxation rate. Calculations have been made and formulas derived for the distance of closest approach using twice the molecular radius.[1] For these haloform molecules distances of closest approach calculated this way did not vary significantly. A distance of closest approach which takes into account the orientational changes between the colliding molecules is needed.

If it is assumed that the molecules are stopped at the instant of interaction, we can say that when the two

molecules are at d, the distance of closest approach, their rotation can be neglected. This should be a good approximation. Figure 2 depicts two molecules with their spins located at f and g. The radius of the molecules, a, can be computed from the molecular volume and $d_o$ is two times the Van der Waals' radius of a hydrogen atom. Trigonometric substitution and manipulation give a value of d which is dependent upon known parameters. If 1/d is integrated from zero to $\pi$ and divided by $\pi$ it gives a value for $\overline{1/d}$ averaged over all relative orientations of the two molecules. The derivation is found in Appendix 1 and the resulting integral is

$$\overline{1/d} = \frac{1}{\pi} \int_o^{\pi} \frac{d\theta}{(2a^2 + 2ad_o + d_o^2 - (2a^2+2ad_o)(\cos\theta))^{1/2}} \qquad (38)$$

The integral was solved by graphical methods. Values of 2.88 Å and 2.95 Å were used for the radii of chloroform and bromoform, respectively. The value used for $d_o$ was 2.40 Å. The results obtained for $\overline{1/d}$ were 0.205 $Å^{-1}$ for the chloroform-bromoform interaction and 0.203 $Å^{-1}$ for the bromoform-bromoform interaction. The results for the interaction between two chloroform molecules for $\overline{1/d}$ was 0.207 $Å^{-1}$. The average distance of closest approach also does not vary significantly for the binary solutions of these two haloforms.

A theoretical model for the relaxation rates of the

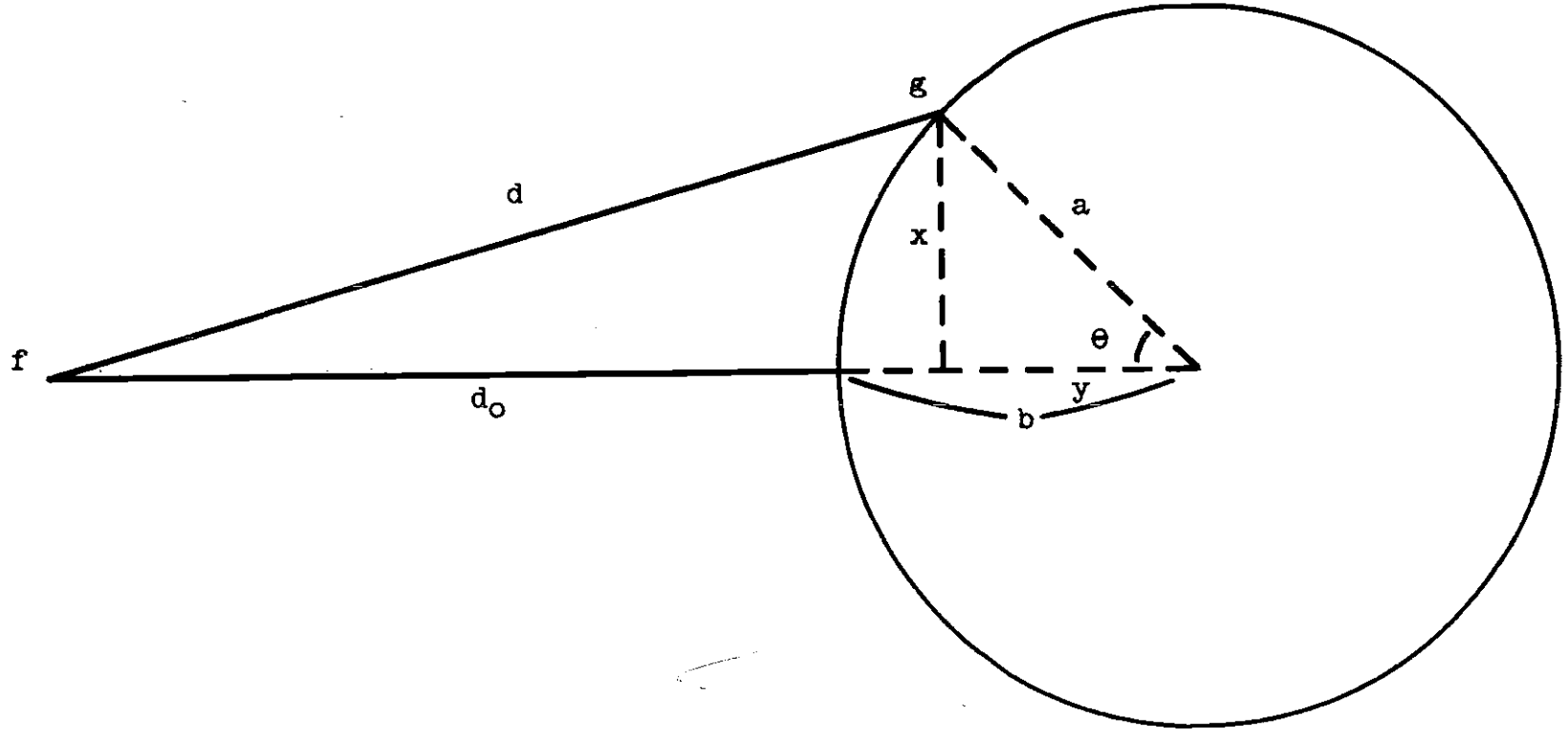


Figure 2. Distance of Closest Approach

molecules in the binary solution can be derived which depends upon the viscosity and the concentrations, if it is assumed that the bromoform-bromoform, bromoform-chloroform, and the chloroform-chloroform interactions are the same. Several assumptions are made. The first is that the viscosity of any particular sample is equal to the sum of the mole fractions times the viscosity of the neat component summed over both components. This is done for simplicity and is valid since the relaxation rate of either component depends upon the viscosity. If all interactions are the same, the viscosity seen is that of the solution, a macroviscosity. A value of 1.741 centipoise was used for neat bromoform and 0.514 was used for the viscosity of neat chloroform.[14] Next, it was assumed that the molar densities of all components were the same. This is justified since the density of bromoform is 0.0114 mole/milliliter and that of chloroform is 0.0124 mole/milliliter. Using the values of neat bromoform relaxation time as 20 seconds and for chloroform 87 seconds, the theoretical curves are constructed. The derivation of the equations for the curves is contained in Appendix 2.

The theoretical curves are shown in Figure 3. The relaxation rate of both components should be equal for all concentrations for experiment B. The relaxation rate of bromoform in experiment A should equal that of neat bromoform initially and then diverge until at infinite dilution

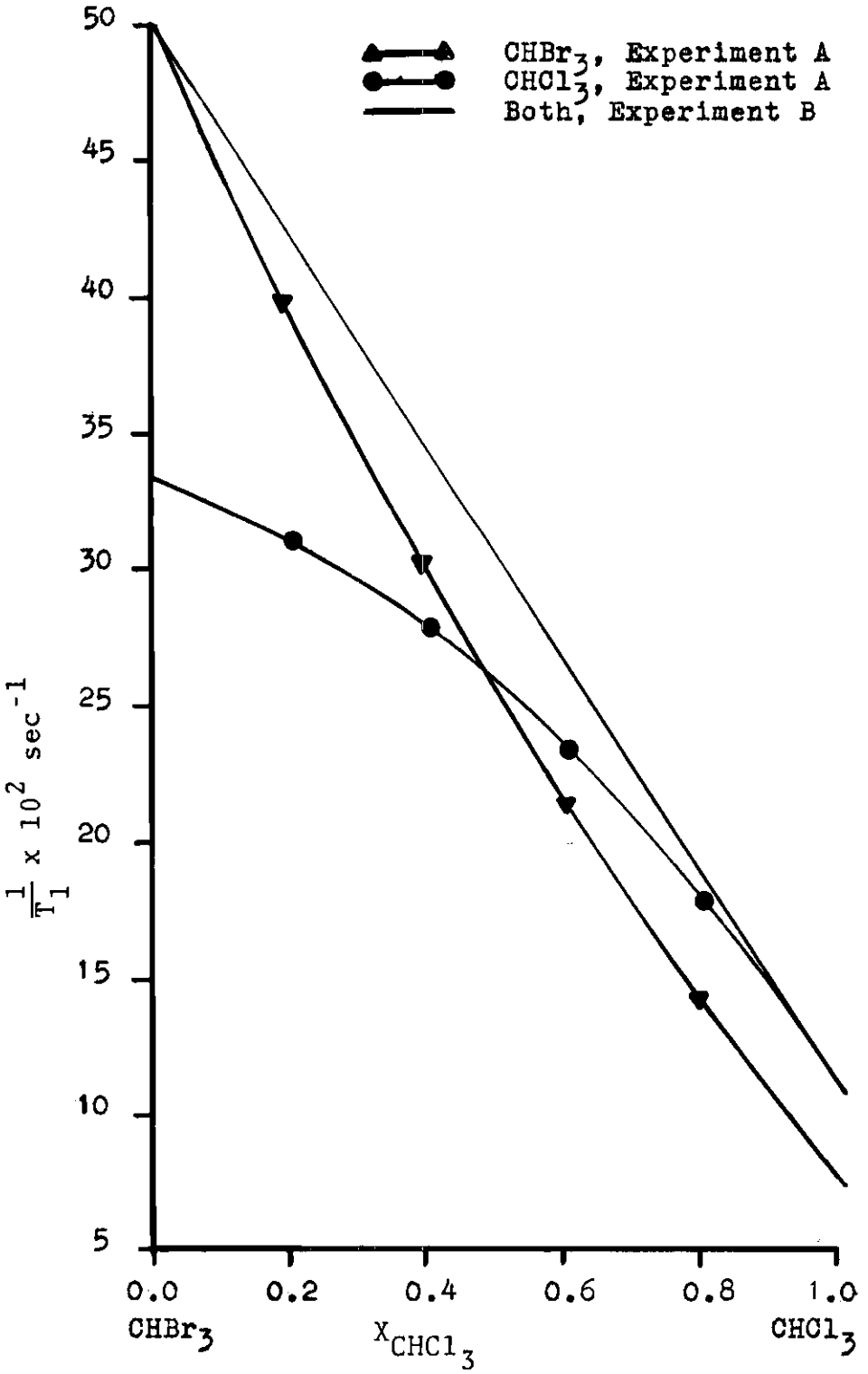


Figure 3. Theoretical Relation Rate Versus Mole Fraction Chloroform

the rate for experiment B is 50% greater than that for experiment A. The chloroform curve follows the same pattern and, as can be seen, should deviate by more as it goes to infinite dilution. At this point, the rate for experiment B is also 50% greater than that of experiment A.

The values of $T_1$ for chloroform dissolved in bromoform were measured for different concentrations. $T_1$ was measured using both experiments. In experiment A, only the chloroform signal was inverted at time zero, and thus the initial relaxation rate is due only to the first term in equation (18). The rates obtained were plotted versus the mole fraction chloroform. In experiment B both the chloroform and bromoform signals were inverted. The relaxation rate then changes because of both terms of equation (18).

The $T_1$ values obtained for both experiments are found in Table 1. The values following the $T_1$'s in parentheses are the average deviations of the six measurements. The corresponding relaxation rates are found in Table 2. The relaxation rate versus the mole fraction of chloroform are given in Figure 4.

The $T_1$ values for bromoform were measured using the same solutions. Bromoform was treated as the solute this time and experiments A and B were performed again. The experimental $T_1$'s are given in Table 3. The corresponding rates are given in Table 4, and the relaxation rate of bromoform versus the mole fraction of bromoform is given in Figure 5.

Table 1. Relaxation Times of Chloroform in Bromoform as a Function of Mole Fraction Chloroform

| Mole Fraction | $T_1$, Sec. (Experiment A) | $T_1$, Sec. (Experiment B) |
|---|---|---|
| 1.00 | 86.1 (±1.6) | 86.1 (±1.6) |
| 0.72 | 70.0 (±1.0) | 66.5 (±1.4) |
| 0.61 | 63.6 (±1.0) | 59.1 (±0.3) |
| 0.46 | 54.0 (±0.6) | 48.6 (±0.8) |
| 0.31 | 43.2 (±1.4) | 39.6 (±1.2) |
| 0.26 | | 34.2 (±0.4) |

Table 2. Relaxation Rates of Chloroform in Bromoform as a Function of Mole Fraction Chloroform

| Mole Fraction | $1/T_1$, $Sec^{-1}$ (Experiment A) | $1/T_1$, $Sec^{-1}$ (Experiment B) |
|---|---|---|
| 1.00 | 0.011 (±.001) | 0.011 (±.001) |
| 0.72 | 0.014 (±.001) | 0.015 (±.001) |
| 0.61 | 0.015 (±.001) | 0.017 (±.001) |
| 0.46 | 0.018 (±.001) | 0.020 (±.001) |
| 0.31 | 0.023 (±.001) | 0.025 (±.001) |
| 0.26 | | 0.029 (±.001) |

Table 3. Relaxation Times of Bromoform in Chloroform as a Function of Mole Fraction Bromoform

| Mole Fraction | $T_1$, Sec (Experiment A) | $T_1$, Sec (Experiment B) |
|---|---|---|
| 1.00 | 20.0 (±0.6) | 20.0 (±0.6) |
| 0.74 | 26.0 (±0.6) | 25.2 (±0.5) |
| 0.69 | 29.3 (±1.6) | 27.4 (±0.5) |
| 0.54 | 36.0 (±2.6) | 31.7 (±0.6) |
| 0.39 | 42.4 (±1.5) | 36.2 (±1.1) |
| 0.28 | 45.1 (±1.4) | 38.6 (±0.7) |

Table 4. Relaxation Rates of Bromoform in Chloroform as a Function of Mole Fraction Bromoform

| Mole Fraction | $1/T_1$, $Sec^{-1}$ (Experiment A) | $1/T_1$, $sec^{-1}$ (Experiment B) |
|---|---|---|
| 1.00 | 0.049 (±.002) | 0.049 (±.002) |
| 0.74 | 0.038 (±.002) | 0.040 (±.001) |
| 0.69 | 0.034 (±.002) | 0.037 (±.001) |
| 0.54 | 0.028 (±.002) | 0.032 (±.001) |
| 0.39 | 0.024 (±.001) | 0.028 (±.001) |
| 0.28 | 0.022 (±.001) | 0.026 (±.001) |

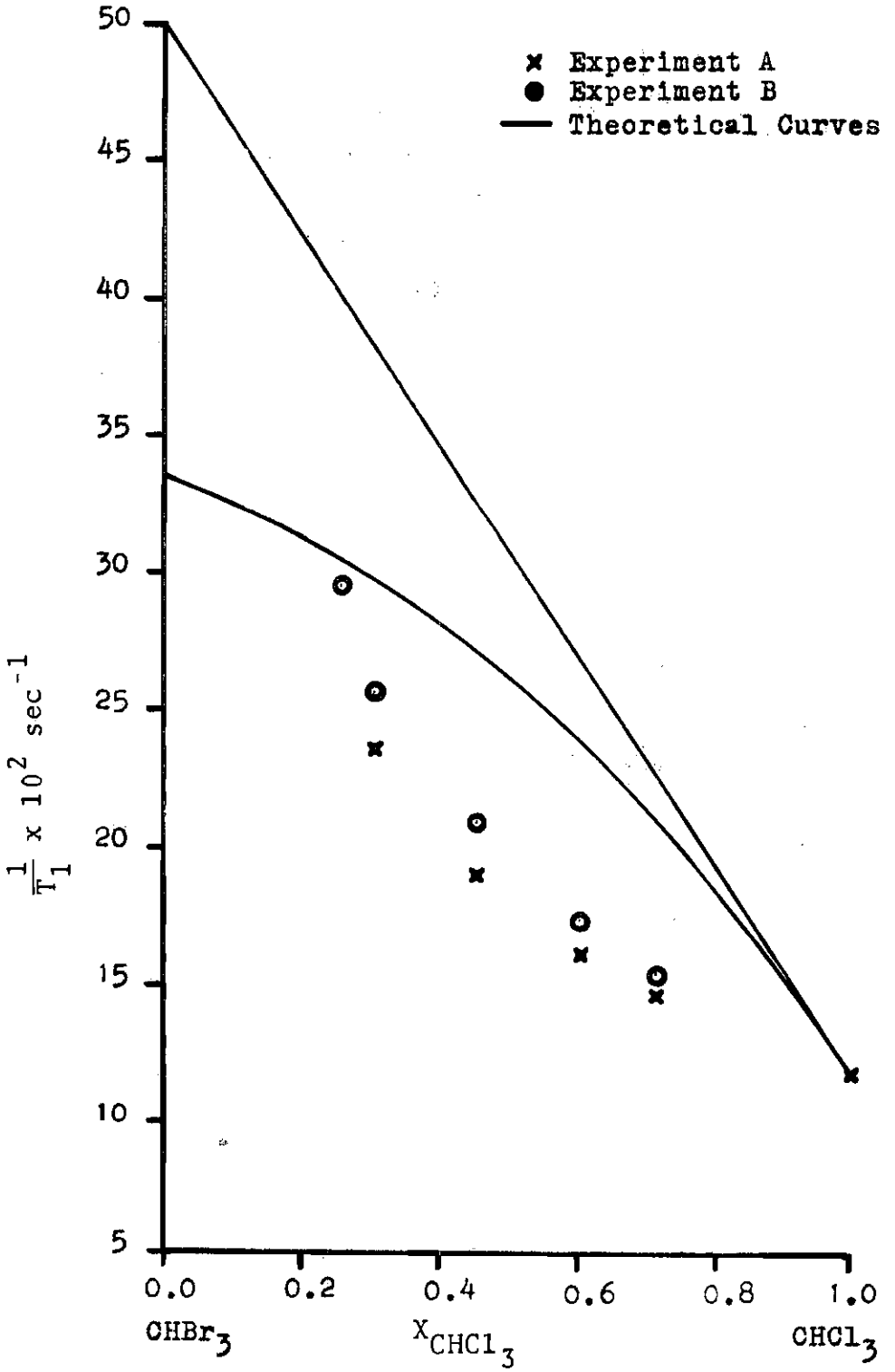


Figure 4. Relaxation Rate of Chloroform Versus Mole Fraction Chloroform

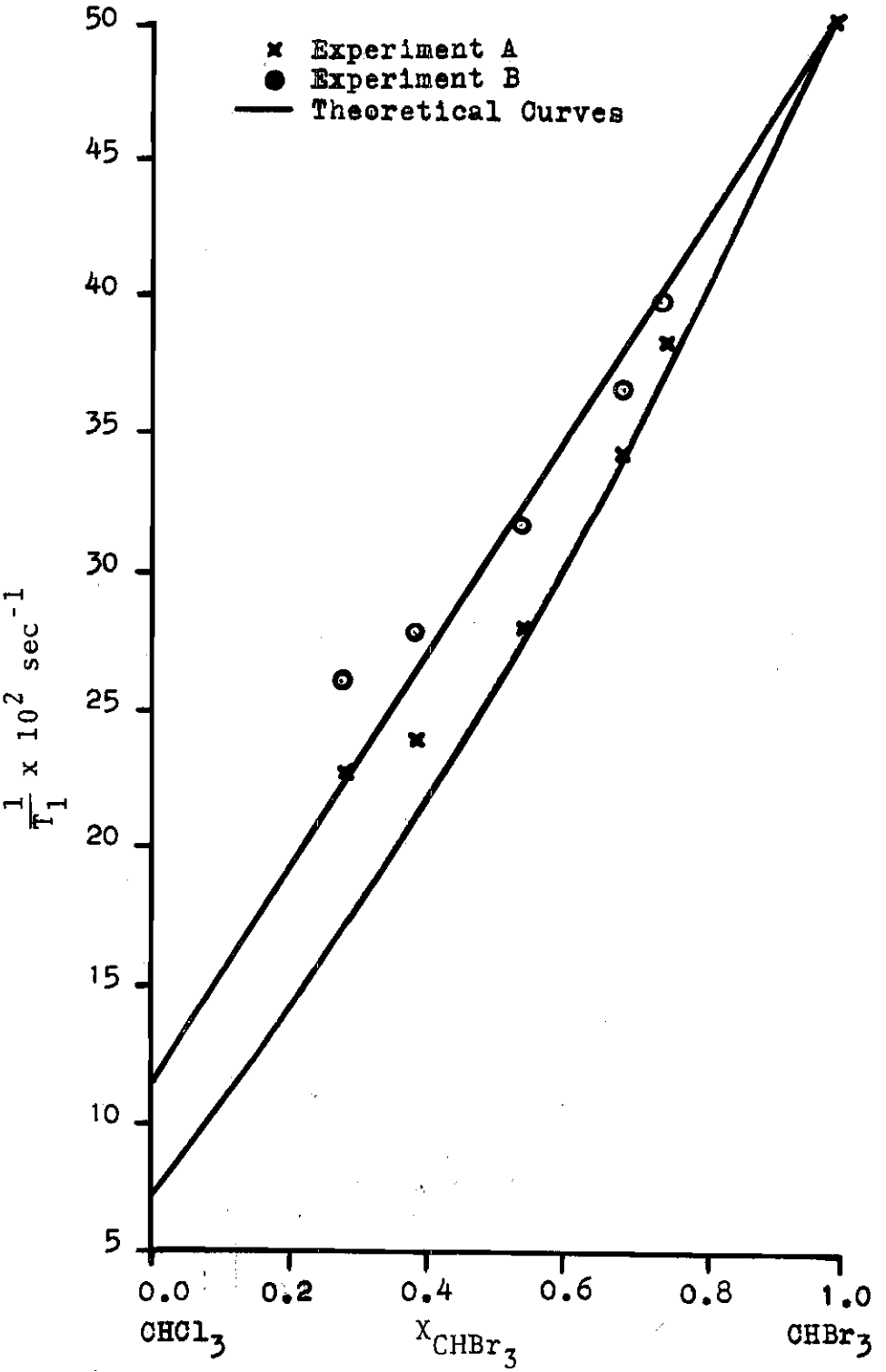


Figure 5. Relaxation Rate of Bromoform Versus Mole Fraction Bromoform

Figure 4 shows that the chloroform results immediately deviated from the theoretical. However it can be seen that as the mole fraction of chloroform decreases the results start curving toward the theoretical. Figure 5 shows the opposite results for the bromoform. These results initially follow the theoretical and start to deviate as the mole fraction of bromoform decreases. In fact, the deviations begin about 0.5 mole fraction. Thus, as the solutions show an abundance of chloroform, they also show deviation from the theoretical results. Thus, the chloroform appears to be causing the deviations from the theoretical.

The theoretical model was developed assuming that the nearest neighbors were determined by the mole fraction. The results show that this is not true. The chloroform could be associating, which would cause it to have more of its own species as nearest neighbors, thus forcing the bromoform to have more of its own species surrounding it. This is why the deviations are seen on the chloroform side. The molecules are obviously not seeing the solution viscosity but a micro-viscosity. Since the rate is proportional to the viscosity, the curves bear this out. The chloroform is seeing a viscosity that is lower than that of the model and thus would fall below the theoretical curve as is seen. The bromoform is seeing a viscosity higher than the model and is above the theoretical curves.

Experimental relaxation times of iodoform were found

for two solutions of iodoform-chloroform performing experiment B only. Samples of 0.025 and 0.031 mole fraction iodoform were used. These results gave rate values which were above those of bromoform which show even more deviation from the theoretical.

These results for iodoform must be regarded as qualitative. The low solubility of iodoform allowed only a small signal to be seen and gave a very poor signal to noise ratio. The experimental $T_1$ of the iodoform was very short not allowing many points to be used for the calculation. This problem compounded by the low signal to noise ratio leaves the data suspect. A way to solve the signal to noise problem would be through the use of proton fourier transform NMR. Unfortunately this capability was not yet operational with the JEOL machine at the time of the experiments.

Since the theoretical curves are for solutions with equal solute-solute, solvent-solvent, and solute-solvent interactions, the results for the bromoform-chloroform solutions show the nonideality of the interactions. Since the interaction is intermolecular only, perhaps the $T_1$ results can be compared to vapor pressure studies. Both the vapor pressure and the intermolecular relaxation rate are dependent upon the interactions with nearest neighbors. Thus, there is possibly a correspondence between the relaxation rate deviations and any deviations the solutions would show from Raoult's Law. The assumptions used for the theoretical

model are similar to those used in deriving Raoult's Law. No data could be found in the literature for the vapor pressure studies of the binary haloform solutions. However, there was data for a chloroform-benzene study. Perhaps a look at this system will tell something about the actions of chloroform in a binary solution.

A vapor pressure curve of a chloroform-benzene binary system shows a positive deviation from Raoult's Law in the region of greater than 0.5 mole fraction chloroform.[15] It would have been expected that a benzene-chloroform pi complex would form and cause a negative deviation from ideality. The curve indicates that the chloroform molecules are associating with other chloroform molecules and this is what causes the positive deviation in this region. The deviation is less than would be expected from what was seen in the relaxation studies because the benzene molecules are competing for the chloroform molecules in order to form the pi complex.

The results for the binary haloform solutions show that information about the molecular interactions can be obtained from relaxation rate studies. Thus, in principle, there could be a comparison with other properties that depend upon intermolecular interactions, and relaxation rates could be used to give quick indications of the trends in these other properties.

# CHAPTER V

## PROTON - CARBON-13 INTERMOLECULAR EXPERIMENTS

A solution of 0.20 mole fraction deuterated acetone in water is a good binary solution to attempt to see a proton - carbon-13 intermolecular Nuclear Overhauser Effect. The carbon-13 spectrum has two major peaks, a carbonyl peak and a methyl peak. This provides an opportunity to look for a differential intermolecular Overhauser effect between the carbonyl and the methyl carbon-13 peaks. The peaks are separated by 4633 Hz. The methyl resonance is a septuplet with splitting of 19.5 Hz. due to the deuterium. The carbon-13 relaxation is more complicated than the binary haloform systems discussed earlier. Since a carbon-13 nucleus is surrounded by a large number of binding electrons, it will have a significant amount of spin rotation relaxation.[16] There will be no intramolecular relaxation due to protons and any relaxation due to the deuterium will be less than 0.024 that which would be expected from normal acetone with protons. This is because the gyromagnetic ratio of the deuteron is 4107 radians second$^{-1}$ Gauss$^{-1}$ as compared to that of the proton which is 26,752.[1] However, there should be intermolecular dipole-dipole relaxation of the acetone carbon-13 due to the protons of the water solvent because of

the large magnetic moment of the proton. A solution of 0.80 mole fraction water solvent was chosen because earlier proton nuclear magnetic resonance studies of acetone-D6 in water at varied concentrations had shown that at approximately 0.8 mole fraction of water the maximum molecular associations occurred.[17]

There is a possibility that the acetone-D6 will exchange with the water under acidic or basic conditions because the methyl is alpha to the carbonyl.[18] The sample used in these experiments was made up at neutral pH, but acidic or basic substances could be leached from the pyrex NMR tube. In order to make sure that the exchange was insignificant, two tests were made.

First, a long term carbon-13 spectrum of the sample was run at room temperature. The sample at this time was approximately 35 days old. Two hundred scans of the spectrum were made with five minutes between scans. This would assure that if a peak had a relaxation time as long as one minute, a period of $5T_1$ was occuring between samplings and no saturation of peaks would occur. It should be noted that a $-CHD_2$ peak would have a relaxation time which would be less than that of a $-CD_3$ peak, which is somewhat less than one minute. However, the five minute repetition time was still used as a precaution. The spectrum obtained was then expanded by fifteen times on the X-axis. The difference between the carbonyl peak locations of acetone and deuterated

acetone is approximately 0.3 ppm.[19] Any exchange of protons for deuterium would cause a shift between zero and this value. The carbonyl peak of the resulting spectrum did not show any shift. The resolution of the spectrometer pen is 0.5 ppm, hence the expansion was used to see if a shift indeed did occur and another peak could be seen. The methyl peak showed no change in its splitting pattern, contrary to what would have been expected if protons had exchanged. The septuplet expanded fifteen times on the X-axis showed no alteration. The exchange of one proton would have given a pattern of two quintets.

The second test run for indications of exchange was to take a proton spectrum of the sample. This was then compared with a proton spectrum of a 0.20 sample of normal acetone in water solvent. The former showed a proton concentration of approximately 0.1% that of the latter.

The nuclear Overhauser experiments will be discussed first. The intramolecular NOE, which has been seen in neat acetone,[16] will not be present because there are no protons to cause it. Therefore any increase in the carbon-13 peak intensities upon irradiation of the proton frequency will be due to an intermolecular interaction. The maximum enhancement that theoretically can occur is 1.99, as can be seen from equation (28).

The sample was sealed in an eight mm NMR sample tube and inserted into a ten mm NMR tube containing carbon

tetrachloride to be used as an external reference. The carbon tetrachloride could not Overhause and could be used as a reference to determine any increase or decrease in the other peaks. A carbon-13 NMR spectrum of the sample was first taken with the decoupler on but with no irradiation of the water protons. This was accomplished by using low power (50 db attenuation) continuous wave decoupling and shifting the frequency of the spin decoupler five thousand Hz. away from the water proton frequency. Then, another spectrum was taken with the frequency of the spin decoupler set at the resonance frequency of the water protons. The temperature of the probe was constant for both experiments at 28° centigrade. The two experiments were performed twice. An earlier attempt to do the experiment by broad band noise decoupling at full power resulted in the probe temperature being raised 16° when the decoupler was on, and gave inconsistent data. This was because the non-decoupled spectrum was taken with the decoupler off and was at 28°.

The results were an enhancement of 0.466 ($\pm$0.028) for the carbonyl carbon-13 and 0.289 ($\pm$0.003) for the deuterated methyl carbon-13 peak. As a check of the stability of the equipment and the magnetic field, a sample of 0.20 mole fraction deuterated acetone in deuterium oxide was run through the same sequence and a deviation of only 0.6% was seen.

Next, the experimental relaxation time for each

carbon-13 of the molecule was determined. The solvent molecules have a greater viscosity than the solute molecules, and thus the acetone should move with more restriction than it does in its neat configuration. Thus if the deuterated acetone has a lower translational velocity, it should have a larger intermolecular relaxation rate. The amount of intermolecular dipolar relaxation can be calculated by using equation (29) and the values for the experimental relaxation rate and the Overhauser enhancement.

The JEOL PFT-100 originally had an automoatic $T_1$ program which took the partially relaxed fourier transform (PRFT) spectrum. It did not compute the $T_1$ value. However the PRFT data could be used to find a value for $T_1$ using the Wang 700 program used for the proton experiments. The results obtained from this $T_1$ program were very erratic and unsatisfactory. It was found that the problem occurred because the PRFT spectrum was taken using a $\pi$-$\pi/2$ pulse sequence whereas the value for the spectrum at thermal equilibrium was taken with a $\pi/2$ pulse method. This resulted in the PRFT spectrum not being phased exactly the same as the $M_\infty$ spectrum. Thus the data was erratic.

A new Auto-$T_1$ program was sent to replace this one which alleviated this problem. The new program used a $\pi$-$\pi/2$ pulse sequence to take the $M_\infty$ spectrum also. The best experimental data is obtained when the $M_\infty$ spectrum is obtained with a wait of $5T_1$ between the $\pi$ and the $\pi/2$

pulses. The maximum wait capability of the digital pulse programmer on the JEOL spectrometer is 99 seconds. The maximum repetition time between the taking of each PRFT, i.e., the time between successive $\pi$ pulses, should also be $5T_1$ but the limitation of the machine was 130 seconds. The implication of this is that data obtained for carbon-13 with long $T_1$ values would be suspect. This problem will be discussed in the interpretation of the $T_1$ values obtained. The new Auto-$T_1$ program also calculated a value for $T_1$ eliminating the need for the Wang program.

The relaxation time obtained for the carbonyl carbon-13 was 38.9 ($\pm$1.6) seconds and for the deuterated methyl carbon-13 it was 51.3 ($\pm$1.1) seconds. These values correspond to rates of 0.0257 second$^{-1}$ and 0.0195 second$^{-1}$, respectively. A closer look at the 130 second wait between repetitions is now warranted. For the methyl peak this means that it only returns to 0.92 $M_\infty$ before the next sequence starts. This will not cause the peak to become saturated, however it does add a factor of error. Also the 99 second wait while determining the value at thermal equilibrium means that the spectrum taken is only 0.86 $M_\infty$. This adds another error factor to the data. The error will be greater in the methyl data since a longer relaxation time was obtained for it.

This experimental relaxation rate can be used with the experimental Overhauser enhancements to calculate the

intermolecular dipolar relaxation rate by equation (29). The dipolar rate for the carbonyl is 0.00599 second$^{-1}$ and for the deuterated methyl is 0.00282 second$^{-1}$. Equation (37) shows that the difference must lie in the diffusion coefficient or the distances of closest approach. It cannot be due to a difference in the relative translational velocities of the different carbon-13 since the molecule is translating as a unit. Thus, the solvent water molecules are interacting more closely with the carbon-13 than with the methyl carbon-13 since the rate is proportional to the inverse of the distance of closest approach. This indicates that the water molecules are more likely to be near the carbonyl carbon than near the deuterated methyl carbon.

It should be noted that the total relaxation rate minus the intermolecular relaxation rate gives the rate due to all other mechanisms. Since only the water proton frequency was irradiated to determine an NOE value, even if considerable proton-deuterium exchange occurred, the intermolecular rate could have been determined since the intramolecular rate would have been included in the rate due to other mechanisms. Thus, in principle, the experiment as performed may be used to obtain intermolecular dipolar relaxation rates even for carbons with directly bonded hydrogen.

# CHAPTER VI

## CONCLUSIONS AND RECOMMENDATIONS

These experiments have shown that the intermolecular dipole-dipole relaxation process in small molecules can be used to give information concerning the molecular collision process in binary solutions. Both proton-proton and proton-carbon-13 interactions have been studied.

The proton-proton studies on the binary haloform solutions have shown that the chloroform molecules are translating faster than would be expected when the solution has an abundance of chloroform. Conversely, the bromoform is translating more slowly than expected. The individual species are not seeing the macroviscosity of the medium but an independent microviscosity. Thus the relaxation rate studies can be said to be probing the microviscosity of each solute.

The ideal model for relaxation could be refined by doing viscosity determinations of the different solutions rather than just assuming a mean viscosity. However, the only difference this would make would be in the general shapes for the ideal curves. The ideal rates for bromoform and chloroform in experiment B would still be equal. Data in the dilute regions would be very helpful in conclusively

determining the absence of spin rotation relaxation in the haloforms and would give an even better look at the interactions occuring between the species.

Because of the signal to noise limitations, data could not be obtained for the binary haloform solutions when the solute concentration was less than about 0.2 mole fraction. Data could be obtained for these regions, however, with a proton fourier transform spectrometer. These experiments would provide data which could be extrapolated to infinite dilution. The extrapolated relaxation rates could then be used to confirm that the relaxation process occuring is entirely dipole-dipole. At infinite dilution the rate for experiment B should be 50% greater than that for experiment A. Data in this region could also be used to see exactly where the chloroform begins to act ideally, as the chloroform approaches infinite dilution. A fourier transform spectrometer would allow the iodoform-chloroform experiments to be done quantitatively and allow similar experiments on iodoform-bromoform. Further studies of the solutions could be done at different temperature in order to determine activation energies for the relative translational motions.

Vapor pressure studies of the chloroform-bromoform solutions could be done and compared with the relaxation results to see if both properties deviate from ideality to the same degree and in the same manner. Proton studies could be done on optical isomers such as ℓ and d sec-Butyl

chloride to see if a solution of equal amounts of each isomer has the same relaxation time as the pure optical isomers. The pure optical isomers should have equal relaxation times since their environments are the same. If it can be seen that a mixture has a different relaxation rate, then relaxation studies could possibly be used to determine intermolecular interactions between optical isomers. A disadvantage to this type of study is that sec-Butyl chloride has more than one proton signal. Systems with one proton or with several protons which have significantly different resonance frequencies would be best for this type of study.

An experiment more along the lines of the binary haloform studies would be to look at a solution of bromoform in 1,2,2-trichloro ethane. Four different experiments could be run while looking at the bromoform relaxation. One when only the bromoform signal is inverted, second with only the bromoform and the $-CHCl_2$ signal inverted, thirdly with only the bromoform and the $-CH_2Cl$ signal inverted, and finally with all of the signals being inverted. The ratio of the increase in the bromoform relaxation rate of the final three experiments over the first one should be 1:2:3, respectively.

The studies of the deuterated acetone-water solution allowed a direct observation of the proton - carbon-13 Nuclear Overhauser Effect for both types of carbon in the acetone molecule. This combined with the relaxation rate

studies of the carbon-13 showed that the solvent molecules were interacting more strongly with the carbonyl portion of the molecule than with the methyl groups.

The capability to select the protons which cause the NOE by using low power continuous wave irradiation could be useful when there are several proton resonances. This would occur in nondeuterated compounds. Studies should be made on normal acetone in water to determine the sensitivity of this type of experiment when there is also the possibility of intramolecular dipolar relaxation.

Measurements of the relaxation rate and NOE could be done at different temperatures in order to measure activation energies. The decrease in the spin rotation relaxation would produce an increase in the NOE. The sample has been taken as low as -20°C without solidifying.

Association studies are perhaps the best use of this type of carbon-13 study. Ketones seem to be a good type of molecule to study since the carbonyl is exposed, and should associate with the solvent more strongly than other parts of the molecule. Other solvents should be used because the solubility of ketones in water decreases with increasing ketone size. Other solvents which have only one type of proton present and could be used are benzene, tetramethylsilane, and dimethyl sulfoxide. The benzene and TMS have one disadvantage in that they have a large number of equivalent carbons.

# APPENDICES

# APPENDICES

A-1 Derivation of equation (38). On Figure 3,

$$d^2 = (d_o + b)^2 + X^2. \tag{A1}$$

In equation (A1), $x = a \sin\theta$, $b = a - y$, and $y = a \cos\theta$. Therefore, $d^2 = (d_o + a(1 - \cos\theta))^2 + a^2 \sin^2\theta$. Then,

$$\frac{\overline{1}}{d} = \frac{1}{\pi} \int_o^{\pi} \frac{d\theta}{(d_o + a(1-\cos\theta)^2 + a^2 \sin^2\theta)^{1/2}}$$

$$= \frac{1}{\pi} \int_o^{\pi} \frac{d\theta}{(d_o^2 + 2ad_o(1-\cos\theta) + a^2(1-2\cos\theta+\cos\theta)+a^2\sin^2\theta)^{1/2}}$$

$$= \frac{1}{\pi} \int_o^{\pi} \frac{d\theta}{(d_o^2 + 2ad_o(1-\cos\theta) + 2a^2(1-\cos\theta))^{1/2}}$$

$$= \frac{1}{\pi} \int_o^{\pi} \frac{d\theta}{(2a^2 + 2ad_o + d_o^2 - (2a^2+2ad_o)(\cos\theta))^{1/2}} .$$

A-2 Derivation of Theoretical Curves of Figure 4.

Equation (18) may be written as

$$dB/dt = -(3/2T_{bb}+1/T_{bc})(B-B_o)-1/2T_{bc}(C-C_o) \tag{A2}$$

and

$$dC/dt = -(3/2T_{cc}+1/T_{cb})(C-C_o) - 1/2T_{cb}(B-B_o). \quad (A2)$$

In equation (A2), $1/T_{bb}$ = Constant $\eta$ $N_b$, where $\eta = \eta_b X_b + \eta_c X_c$. Therefore, $1/T_{bb}$ = Constant $\eta_b(X_b + \eta_c X_c/\eta_b)X_b$. it is assumed that $N_b + N_c = N_o$. Then,

$$1/T_{bb} = \text{Constant } N_o\ \eta_b\ (X_b + \eta_c X_c/\eta_b)X_b.$$

Next, it is assumed that $\eta_c/\eta_b = T_b^o/T_c^o$. Then,

$$1/T_{bb} = \text{Constant } N_o\ \eta_b\ (X_b + T_b^o X_c/T_c^o)X_b.$$

When $X_b = 1$,

$$1/T_{bb} = 1/T_b^o, \text{ where } 1/T_1 \text{ (of neat B)} = 3/2T_b^o.$$

Thus, $1/T_b^o$ = Constant $\eta_b$ $N_o$, and

$$1/T_{bb} = 1/T_b^o(X_b + T_b^o X_c/T_c^o)X_b = (X_b/T_b^o + X_c/T_c^o)X_b/$$

Similarly,

$$1/T_{cb} = 1/T_{bb} = (X_b/T_b + X_c/T_c)X_b = 1/T_b$$

and

$$1/T_{cc} = 1/T_{bc} = (X_b/T_b + X_c/T_c)X_c = 1/T_c.$$

Therefore,

$$dB/dt = -(3/2T_b + 1/T_c)(B-B_o) -1/2T_c(C-C_o)$$

and

$$dC/dt = -(3/2T_c + 1/T_b)(C-C_o) -1/2T_b(B-B_o).$$

For Experiment A,

$$(1/T_1)_b = 3/2T_b + 1/T_c, \tag{A3}$$

$$(1/T_1)_c = 3/2T_c + 1/T_b. \tag{A4}$$

For Experiment B,

$$(1/T_1)_b = \frac{3}{2}\,(1/T_b + 1/T_c) = (1/T_1)_c. \tag{A5}$$

The curves in Figure 4 were obtained by plotting A3, A4, and A5 versus $X_{CHCl_3}$, with $T_A^o = 87$ and $T_A^o = 20$.

# LITERATURE CITED*


1. J. H. Noggle and R. E. Schirmer, The Nuclear Overhauser Effect, Academic Press, New York, 1971.

2. T. L. Prendred, A. M. Pritchard, and R. E. Richards, J. Chem. Soc. A., 1009 (1966).

3. N. R. Krishna and S. L. Gordon, Unpublished Results.

4. N. R. Krishna and B. D. N. Rao, Mol. Phys. 22, 937 (1971).

5. N. Bloembergen, E. Purcell, and R. V. Pound, Phys. Rev., 73, 679 (1948).

6. A. Abragam, The Principles of Nuclear Magnetism, Oxford University Press, London, 1961.

7. G. C. Levy and G. L. Nelson, Carbon-13 Nuclear Magnetic Resonance for Organic Chemists, Wiley Interscience, New York, 1972.

8. I. Solomon, Phys. Rev., 99, 599 (1955).

9. H. S. Gutowsky and D. E. Woessner, Phys. Rev., 104, 843 (1956).

10. A. Gierer and K. Wirtz, Z. Naturforsch A8, 532 (1953).

11. J. A. Pople, W. G. Schneider, and H. J. Bernstein, High Resolution Nuclear Magnetic Resonance, McGraw Hill, New York, 1959.

12. T. C. Farrar and E. D. Becker, Pulse and Fourier Transform NMR, Academic Press, New York, 1971.

13. Manufacturers Literature, Japan Electron Optics Laboratory Co., Ltd. (USA), 238 Brichwood Avenue, Cranfield, New Jersey, 07016, 1973.

14. The Chemical Rubber Co., Handbook of Chemistry and Physics, 51st Edition, The Chemical Rubber Publishing Company, Ohio, 1970.


*Journal title abbreviations used are listed in "Index of Periodicals," Chemical Abstracts, 1970.

15. J. Timmermans, The Physico-chemical Constants of Binary Systems in Concentrated Solutions, Vol. 1, Interscience Publishers, Inc., New York, 1959.

16. T. C. Farrar, S. J. Druck, R. R. Shoup, and E. D. Becker, J. Amer. Chem. Soc., 94, 699 (1972).

17. L. W. Reeves and C. P. Yue, Can J. Chem., 48, 3307 (1970).

18. H. M. Dawson and E. Spivey, J. Chem. Soc., 2180 (1930).

19. G. E. Maciel, P. D. Ellis, and D. C. Hofer, J. Phys. Chem., 71, 2160 (1967).